

## **P-S polarity reversal: is it always at zero offset?**

M. Graziella Kirtland Grech, Don C. Lawton, Robert R. Stewart, Saul E. Guevara and Gary F. Margrave

### **ABSTRACT**

Two numerical seismic modeling experiments have been carried out to investigate whether the polarity reversal on 2D P-S data always occurs at zero-offset. The models included divergent reflectors and a depth-variant  $V_p/V_s$ . The modeling results showed that there are situations where the polarity change of P-S events on the in-line geophone will not be at zero-offset. For a  $V_p/V_s$  that decreased with depth, the displacement of the normal incidence P-S ray from zero-offset was in the up-dip direction. This displacement was in the range of 50 - 200 m for dips up to  $22.5^\circ$  and reflection depths less than 2500 m, but in rare geological situations where the dip was up to  $60^\circ$ , it was found to be as high as 550 metres for a reflection depth of 2100 m. When the interface was flat, the polarity reversal occurred at zero-offset.

### **INTRODUCTION**

Shoshitaishvili et al., (2000) pointed out that in the case of depth-varying  $V_p/V_s$ , normal incidence and polarity reversal of P-S raypaths does not occur at zero-offset. In fact they observed polarity reversals at offsets as large as 2000 m on synthetic gathers. If ignored, this polarity reversal will affect residual curvature estimation during semblance analysis, and hence the stack quality (Shoshitaishvili et al., 2000).

In this study, the concept of normal incidence and polarity reversal at non zero-offset was tested with two simple models containing divergent reflectors and  $V_p/V_s$  that varies with depth, generally high to low. In extreme geological situations, where the dip is very steep and  $V_p/V_s$  decreases with depth, polarity reversal at non-zero offset was observed at a distance of a few hundred metres from zero-offset.

### **THE NUMERICAL MODELING EXPERIMENTS**

Two models were built. Model 1 consisted of 4 interfaces (Figure 1) - one flat and three dipping, making angles of  $5^\circ$ ,  $10^\circ$  and  $15^\circ$  with the horizontal, respectively. The P- and S-wave velocities for each layer, together with the corresponding  $V_p/V_s$  are given in Table 1. Acquisition geometry was of the split-spread type, with thirty-six receivers on either side of the spread. The receiver interval was 50 m. Only one shot was acquired and this was located at 6200 m. The thickness of each layer vertically beneath the shot was 500 m in each case.

Model 2 (Figure 2) also consisted of 4 interfaces, the first one was flat, and the other three made an angle of  $22.5^\circ$ ,  $45^\circ$  and  $60^\circ$  with the horizontal, respectively. A split-spread configuration was again used for acquisition. There was a total of sixty channels, thirty on either side of the spread, with a receiver interval of 50 m. One shot was acquired, located at 4000 m. The P- and S-wave velocities and  $V_p/V_s$  for this

model are the same as for model 1 (Table 1). The density for each layer in both models was  $2300 \text{ kg/m}^3$ .

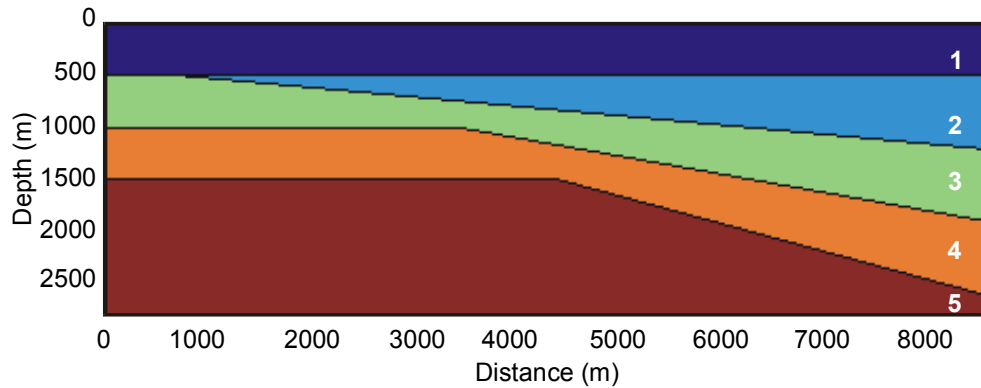


Figure 1. The first model, showing one flat layer and three dipping layers making angles of  $5^\circ$ ,  $10^\circ$  and  $15^\circ$  with the horizontal respectively.  $V_p/V_s$  increases with depth.

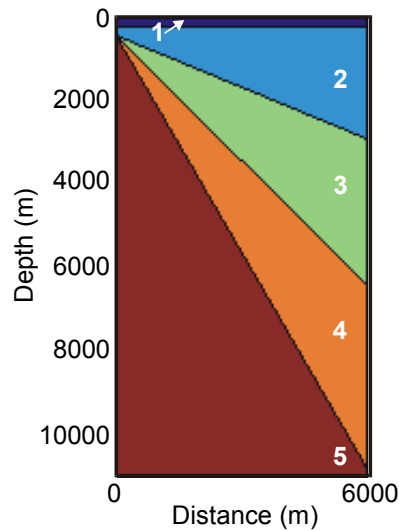


Figure 2. Like model 1, this model also consists of one flat layer and three dipping interfaces, but in this case the dips are steeper. The angles of the three dipping interfaces with the horizontal are  $22.5^\circ$ ,  $45^\circ$  and  $60^\circ$  respectively.

| Layer Number | $V_p$ (m/s) | $V_s$ (m/s) | $V_p/V_s$ |
|--------------|-------------|-------------|-----------|
| 1            | 1600        | 400         | 4         |
| 2            | 1800        | 600         | 3         |
| 3            | 2000        | 800         | 2.5       |
| 4            | 2200        | 1100        | 2         |
| 5            | 2400        | 1300        | 1.8       |

Table 1. P-wave and S-wave velocities and the corresponding  $V_p$  to  $V_s$  ratio for each layer in model 1 and model 2.

### Ray-tracing and synthetic seismogram generation

A general ray-tracing program developed by Kirtland Grech and Lawton (1999) was used to perform the P-S ray tracing and generate the synthetic seismograms. Ray-tracing was done from each interface in both models. The P-S raypaths for the reflector between layers 4 and 5 for model 1 are shown in Figure 3 and those for model 2 in Figure 4. Synthetic seismograms showing the resulting P-S reflections from each of the 4 interfaces are shown in Figure 5 for model 1 and Figure 6 for model 2.

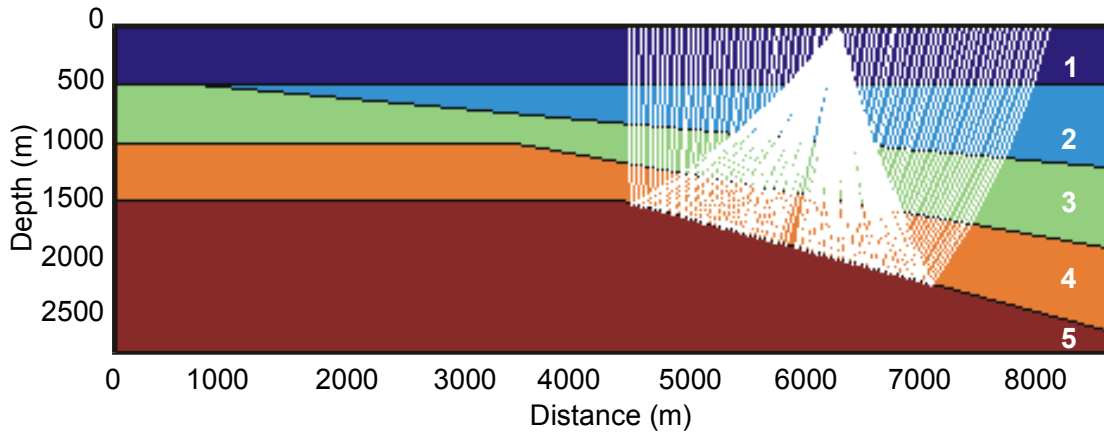


Figure 3. P-S raypaths for interface 4 (model 1). Shot was located at 6200 m.

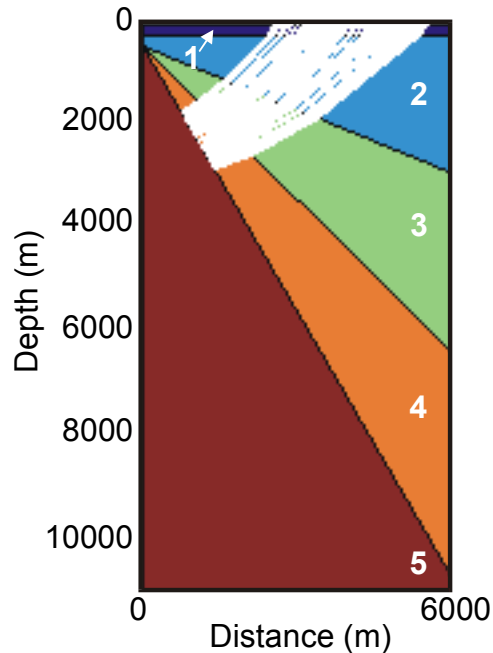


Figure 4. P-S raypaths for interface 4 (model 2). Shot located at 4000 m.

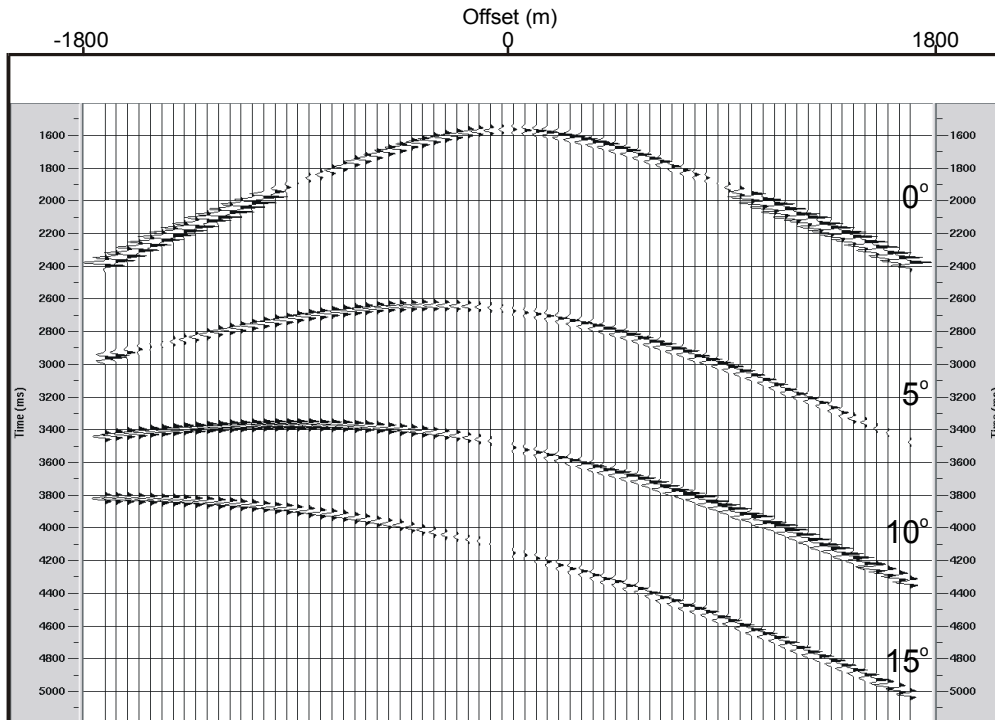


Figure 5. Synthetic seismogram showing reflections from each of the four interfaces in model 1 (the dip of each interface is annotated next to its corresponding reflection).

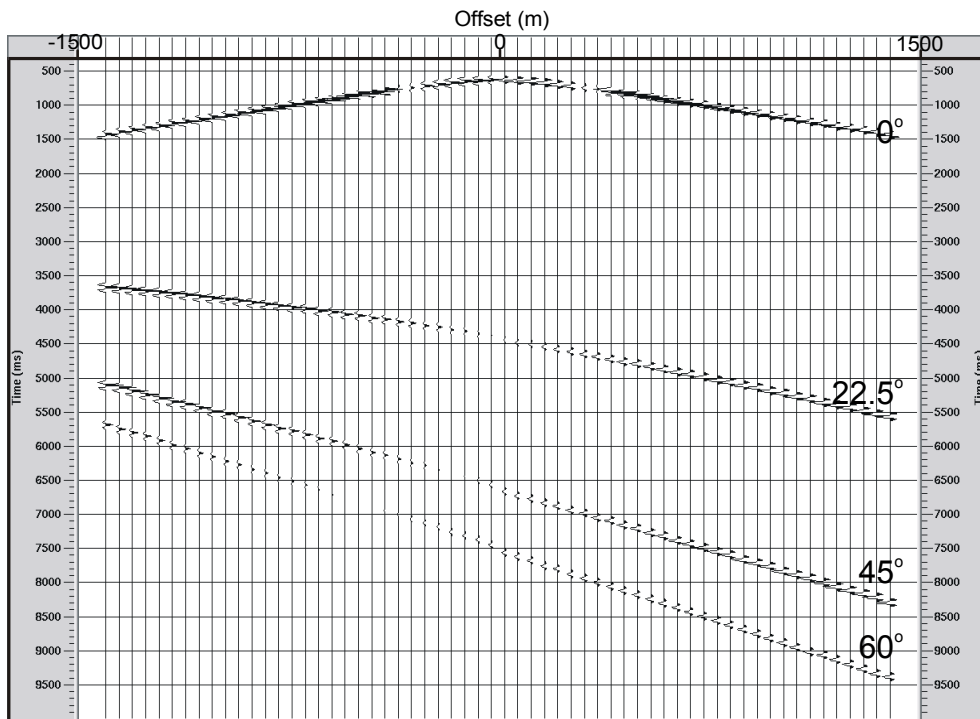


Figure 6. Synthetic seismogram showing reflections from each of the four interfaces in model 2 (interface dips are annotated next to the corresponding reflection).

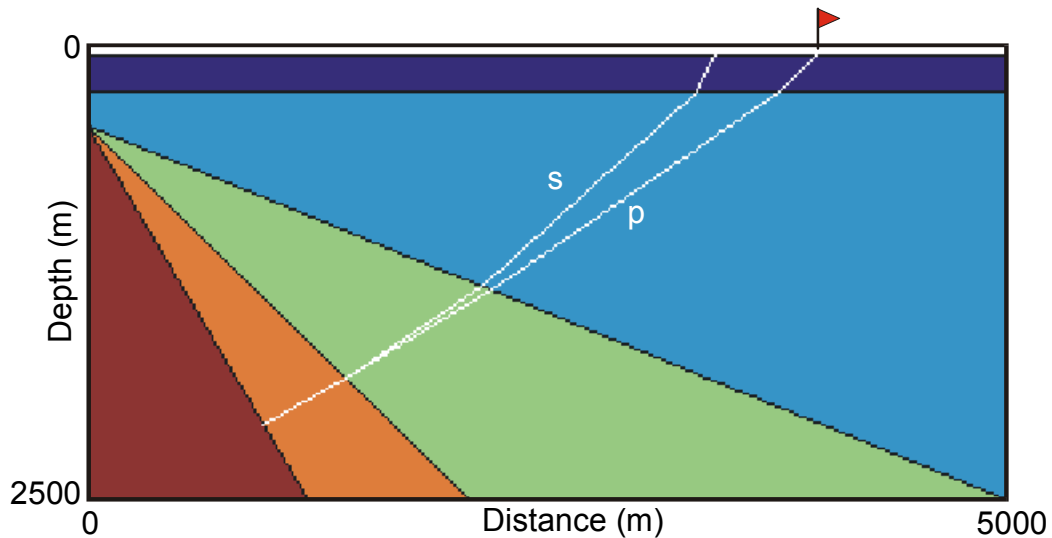


Figure 7. P-S raypath for a receiver at 3450 m and a shot at 4000 m (model 2). The shot location is marked with a red flag). Note how the downgoing P-wave is at normal incidence on the 4<sup>th</sup> interface, whereas the reflected S-wave refracts away from the downgoing P-raypath as it travels back to the surface. The amplitude at the receiver is zero.

## RESULTS

Close examination of Figure 5 (synthetic seismogram for model 1) reveals that the polarity change is exactly at zero-offset for the flat layer and moves away from zero-offset with increasing dip. For the 5° dip interface, it is between 0 and 50 m, for the 10° interface, it occurs at about 50 m (one trace away from zero-offset) and for the 15° dip interface, it occurs at a distance slightly greater than 50m. For model 2 (Figure 6), the polarity change occurs at zero-offset for the flat interface, between 0 and 50 m for the shallow-dipping (22.5°) interface, whereas it is displaced from zero-offset in the up-dip direction by 200 m and 550 m for the steeper interfaces (45° and 60°) respectively. It is important to distinguish polarity changes caused by normal-incidence P-S geometry from polarity changes caused by post-critical incident P-waves, as shown on the far offsets of the early events in Figure 5.

The case of a ‘zero-amplitude’ conversion point away from zero-offset is illustrated in Figure 7. It shows the P-S raypath for a receiver at location 3450 m (model 2), that is at an offset of 550 m from the shot, which is located at 4000 m. The downgoing P-wave is at normal incidence upon the reflector. In this case the reflected S raypath (although this wave has zero-amplitude) will refract away from the downgoing P raypath as it passes through overlying interfaces. The latter have a contrast in  $V_p/V_s$  and are not parallel to the reflector.

## CONCLUSION

Structural geometry and a change in  $V_p/V_s$  with depth may result in a P-S polarity change on P-S data that is not at zero-offset. In general, this will lie within 50 - 200 m of zero-offset for dips up to 22.5° and reflection depths less than 2500m, and will likely be included in an inside mute applied during processing. In some cases of

rapidly increasing dip, however, the polarity change may occur at a significant distance from zero-offset. In fact, for a dip of  $60^\circ$  and reflection depth of about 2100 m, the polarity reversal occurred at an offset of 550 m in the up-dip direction from the shot location. In these cases, the best approach to data processing would be prestack depth migration with a phase correction applied as the event is mapped along the aplanatic surface.

### **ACKNOWLEDGMENTS**

We thank Veritas GeoServices Ltd., sponsors of CREWES and the Fold-Fault Research Project and NSERC for their financial support. Thanks go to Oleg Mikhailov, Elena Shoshitaishvili and their colleagues for bringing up this concept at the SEG/EAGE summer workshop, held in Boise, Idaho between October 1-6, 2000, from which this study was inspired.

### **REFERENCES**

- Kirtland Grech, M.G. and Lawton D.C., 1999, Potential for imaging in fold and thrust belts using multimode events: FRP research report, **5**, 6.7-6.14.
- Shoshitaishvili, E., Mikhailov, O. and Frasier, C.W., 2000, Pre-stack depth migration workflow for converted waves, *in* Recent advances in shear wave technology for reservoir characterization: A new beginning? Proceedings of the SEG/EAGE summer research workshop, Boise, Idaho, October, 1-6, 2000.